CERN-INTC-2023-020 / INTC-P-608-ADD-1
11/01/2023

EUROPEAN ORGANIZATION FOR NUCLEAR RESEARCH

Addendum to the ISOLDE and Neutron Time-of-Flight Committee

IS702: Probing the doubly magic shell closure at ^{132}Sn by Coulomb excitation of neutron-rich ^{130,134}Sn isotopes

January 11, 2023

P. Reiter[1], Th. Kröll[2], M. Droste[1], K. Arnswald[1], A. Blazhev[1], H. Hess[1], H. Kleis[1], D. Mücher[1], N. Warr[1], C. Henrich[2], L. Atar[2], A.-L. Hartig[2], H.-B. Rhee[2], M. von Tresckow[2], C. Sürder[2], I. Homm[2], N. Pietralla[2], M. Scheck[3], R. Gernhäuser[4], H. De Witte[5], M. Huyse[5], P. Van Duppen[5], P. Thirolf[6], L. P. Gaffney[7], A. Jungclaus[8], K. Wimmer[9], M. Gorska-Ott[9], G. Georgiev[10], K. Stoychev[10], J. Cederkäll[11], G. Rainovski[12], D. Kocheva[12], K. Gladnishki[12], D. Bucurescu[13], N. Mărginean[13], R. Mărginean[13], D. Deleanu[13], A. Negret[13], D. Balabanski[14], K. Hadynska-Klek[15], K. Wrzosek-Lipska[15], P. J. Napiorkowski[15], M. Komorowska[15], A. Korgul[15], V. Bildstein[16], R. Chapman[3], T. Grahn[17,18], P. T. Greenlees[17,18], J. Pakarinen[17,18], P. Rahkila[17,18], R. Lozeva[19], A. Andreyev[20], L. M. Fraile[21], A. Illana[21], J. A. Briz[21], M. Llanos[21], J. Benito[21,25], J. M. Allmond[22], A. Stuchbery[23], F. Browne[24], and the MINIBALL and HIE-ISOLDE collaborations

[1] *Univ. of Cologne, Germany*; [2] *TU Darmstadt, Germany*; [3] *Univ. West of Scotland, Paisley, UK*; [4] *TU München, Germany*; [5] *KU Leuven, Belgium*; [6] *LMU München, Germany*; [7] *Univ. of Liverpool, UK*; [8] *IEM CSIC, Madrid, Spain*; [9] *GSI, Darmstadt, Germany*; [10] *IJCLab, Orsay, France*; [11] *Univ. of Lund, Sweden*; [12] *Univ. of Sofia, Bulgaria*; [13] *IFIN-HH, Bucharest, Romania*; [14] *ELI-NP, Măgurele, Romania*; [15] *Heavy Ion Laboratory, Univ. of Warsaw,Poland*; [16] *Univ. of Guelph, Canada*; [17] *Univ. of Jyväskylä, Finland*; [18] *Helsinki Institute of Physics, Finland*; [19] *IJCLab, Université Paris-Saclay, Orsay, France*; [20] *Univ. of York, UK*; [21] *UC Madrid, Spain*; [22] *Oak Ridge National Laboratory, USA*; [23] *Australian National University, Canberra, Australia*; [24] *ISOLDE, CERN, Genève, Switzerland*; [25] *INFN, Sez. di Padova, Italy*

Spokespersons: P. Reiter [preiter@ikp.uni-koeln.de], Th. Kröll [tkroell@ikp.tu-darmstadt.de]
Contact person: F. Browne [frank.browne@cern.ch]

Abstract: In this addendum to experiment IS702, we propose to study the isotope ^{134}Sn by γ-ray spectroscopy following "safe" Coulomb excitation. It is part of our programme to investigate electromagnetic properties of even-even tin isotopes around the doubly-magic ^{132}Sn which started with IS551 (^{132}Sn) and continued with the first part of IS702, the study of ^{130}Sn. The latter has been performed in November 2022 as

first experiment with the upgraded Miniball after LS2. Our investigation of the evolution of the collectivity around the doubly-magic shell closures at $N = 82$ and $Z = 50$ is based on the determination of reduced transition strengths, in particular the $B(E2; 0^+_{\text{g.s.}} \rightarrow 2^+_1)$ values. In addition, the determination of electric quadrupole moments Q_2 and, potentially, $B(E3)$ values is possible. The results challenge the most advanced shell-model calculations using realistic interactions. ^{130,134}Sn with only two neutrons more or less with regard to the closure at $N = 82$ are the key nuclei for the understanding of the nuclear structure in this region.

Requested shifts: [15+3] shifts
Installation: [MINIBALL + CD (C-REX)]

1 Motivation and Physics Case

The two doubly magic nuclei ^{100}Sn and ^{132}Sn are subject of great and persisting experimental as well as theoretical interest. Moreover, the region around ^{132}Sn is the focus of many efforts since the astrophysical r process is expected to pass through this region. The understanding of the nuclear structure has an impact on the description of the $A \approx 130$ peak in the solar element abundances[1].
Advanced techniques and new facilities using radioactive ion beams, allow to obtain new data which offer the opportunity to test recent theoretical models. Latest state-of-the-art Monte-Carlo Shell-Model (MCSM) calculations are performed with an unprecedented large configuration space with eight single-particle orbits for protons and neutrons [2]. This calculation allowed a detailed description of the shape evolution along the tin isotopic chain between $^{100-138}$Sn with one fixed Hamiltonian.

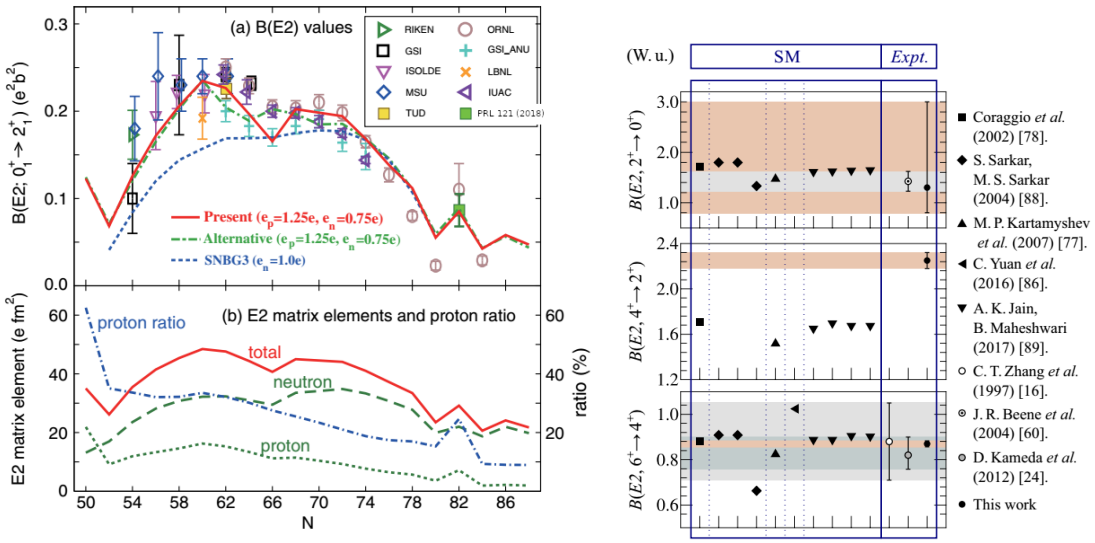

Figure 1: (left) The $B(E2, 0^+_{\text{g.s.}} \rightarrow 2^+_1)$ systematics for the Sn isotopes (status of 2018, figure from Ref. [2]): (a) measured (symbols) and calculated $B(E2)$ values and (b) $E2$ matrix elements and proton ratio (%); (right) Experimental values and theory predictions for $B(E2, I^+ \rightarrow (I-2)^+)$ values in ^{134}Sn (figure from Ref. [3], Refs. therein).

The left panel of Fig. 1 summarises the knowledge of experimental reduced transition strengths $B(E2, 0^+_{\text{g.s.}} \rightarrow 2^+_1)$ and theory predictions by large scale SM calculations from Ref. [2] along the tin isotopic chain. The data points for unstable nuclei are obtained from Coulomb excitation using radioactive ion beams. The new value for ^{134}Sn from a lifetime measurement applying the fast-timing technique is included in the right panel of Fig. 1. Remarkably, below $N = 82$ nearly all the calculated $B(E2, 0^+_{\text{g.s.}} \rightarrow 2^+_1)$ values follow closely the experimental values within their experimental uncertainties. In this way, the long term problem of the enhanced quadrupole collectivity on the neutron-deficient side (see for example Refs. [4, 5, 6]) and the non-parabolic behaviour of these $B(E2)$ values was resolved. As the $Z = 50$ gap is large and almost constant over a wide mass range,

[1] In 2017, for the first time observations confirmed a binary neutron star merger as an astrophysical site of the r-process with the light curves as indicator for the composition of isotopes produced and their decay [1].

proton excitations across it require large excitation energy. The first 2_1^+ levels of Sn have excitation energies of ∼1.2 MeV and vary only smoothly along the whole Sn chain between the two doubly-magic Sn isotopes. The wave function of the 2_1^+ states is dominated by neutron excitations (Fig. 1, bottom of left panel). The small rise and fall of the state around $N = 64$ is caused by the presence of a weak sub-shell closure. The constancy of the 2_1^+ energies at each side of the sub-shell closure confirms that pairing correlations dilute shell occupancies and generate 2_1^+ states of similar configurations. For $82 > N > 66$, the $B(E2)$ values follow the parabolic trend of the generalized seniority scheme.

However, at ^{132}Sn, both proton and neutron low-energy excitations are hindered due to the presence of shell gaps. The increase of the excitation energy of the 2_1^+ state, $E(2_1^+)$, for ^{132}Sn nucleus arises from the fact that both neutron and proton excitations across the $Z = 50$ and $N = 82$ shell gaps require high energies. Therefore, the ^{132}Sn nucleus exhibits the characteristics of a doubly-magic nucleus with a high energy for the first excited states. The mixed wave function of the 2_1^+ state has a larger proton ratio causing the local increase of the $B(E2)$ value with respect to the neighbouring even-even isotopes. For ^{132}Sn, a recent experiment (IS551) performed at HIE-ISOLDE with the MINIBALL & C-REX set-up has revealed enhanced $E2$ and $E3$ strengths [7]. The measured $B(E2)$ value of 0.087 e^2b^2 compares well with the theoretical value of 0.085 e^2b^2 [2].

Beyond the $N = 82$ shell closure, the neutron excitations dominate again. It is noteworthy that $E(2_1^+)$ in ^{130}Sn is 1221 keV while in ^{134}Sn it is only 725.6 keV. In contrast, the measured $B(E2; 0_{\rm gs}^+ \rightarrow 2^+)$ value of 0.029(5) e^2b^2 for ^{134}Sn is very similar to the value of 0.023(5) e^2b^2 for the two-hole nucleus ^{130}Sn [8, 9, 10]. The Tokyo shell-model group calculates larger $B(E2, 0_{\rm g.s.}^+ \rightarrow 2_1^+)$ values of 0.055, 0.044 and 0.056 e^2b^2 for ^{130}Sn, ^{134}Sn and ^{136}Sn, respectively [2].

The left panel of Fig. 1 also clearly reveals that the agreement between experiment and SM model is worst for ^{130,134}Sn, hence for both direct even-even neighbours of the doubly-magic ^{132}Sn. The experimental $B(E2)$ values shown in the figure for these two isotopes are preliminary results which were published only in conference proceedings [8, 9, 10], not in peer-reviewed journals. Therefore the determination of reliable experimental values in particular for these isotopes, the aim of experiment IS702, is of uppermost importance.

The great interest in this region on the theory side is evidenced also by several other approaches which are summarised in the following:

Recent large-scale shell-model calculation including the large model space spanned by $0h_{11/2}$, $1f_{7/2}$, $0h_{9/2}$, $1f_{5/2}$, $2p_{3/2}$, $2p_{1/2}$ orbitals for neutrons, and $0g_{9/2}$, $0g_{7/2}$, $1d_{5/2}$, $1d_{3/2}$, $2s_{1/2}$ orbitals for protons above the inert core of ^{110}Zr, were performed by N. Houda and F. Nowacki from the Université de Strasbourg. The $B(E2, 0_{\rm g.s.}^+ \rightarrow 2_1^+)$ strengths from this large-scale shell-model calculation yield 0.028 and 0.027 e^2b^2 for ^{130}Sn and ^{134}Sn, respectively. Both agree with the preliminary experimental values.

Predictions for neutron-rich Sn nuclei were also made employing a separable quadrupole-plus-pairing Hamiltonian and the Quasi-Particle Random-phase Approximation (QRPA) [11]. Excitation energies, $B(E2, 0_{\rm g.s.}^+ \rightarrow 2_1^+)$ strengths, and g factors for the first 2_1^+ states near ^{132}Sn ($Z > 50$) were calculated. A local maximum of the $B(E2, 0_{\rm g.s.}^+ \rightarrow 2_1^+)$ value at $N = 82$ and a symmetric behaviour for the $N = 80, 84$ neighbours is predicted. For the ^{130,132,134}Sn isotopes the theoretical $B(E2)$ values are also considerably lower than the preliminary determined experimental values.

Another important aspect of studies in this region is related to the long-standing problem of how accurate the description of nuclear structure is provided by realistic shell-model interactions employing two-body matrix elements deduced from a realistic nucleon-nucleon interaction. This is considered a more fundamental approach to the nuclear shell model than the calculations which are based on empirical effective interactions containing several adjustable parameters. Various approaches have been used to generate shell-model interactions capable to predict properties of neutron-rich nuclei beyond $N = 82$ using either empirical approaches (e.g. SMPN) [12] or realistic free nucleon-nucleon potentials (e.g. CD-Bonn), renormalized by either G-matrix (e.g. CWG) [13] or $V_{low\,k}$ methods [14]. For Sn isotopes, the calculations with empirical interactions predict even a new shell closure at $N = 90$ as the $\nu f_{7/2}$ orbital is filled, whereas the calculations with realistic interactions do not find such an effect. The $\nu f_{7/2}$ orbit being filled beyond $N = 82$ shows an interesting analogy with the Ca isotopic chain where a $\nu f_{7/2}$ orbital is filled between $N = 20$ and $N = 28$. There was the long-standing problem that realistic interactions were not able to reproduce the shell closure at $N = 28$. This has been resolved by including three-body forces [15]. Indeed, a shell closure at $N = 90$ in ^{140}Sn is predicted including three-body forces by calculations based on realistic interactions (CWG3M) [16].
To judge the predictive power of new calculations at this critical position in the chart of nuclei, new measurements with high accuracy are needed. Therefore, we propose to extend our studies by γ-ray spectroscopy following 'safe' Coulomb excitation to the isotope ^{134}Sn in order to obtain a reliable $B(E2, 0^+_{\text{g.s.}} \rightarrow 2^+_1)$ value and to complete the experimental data set which will allow for resolving the puzzling discrepancy for the crucial isotopes ^{130,134}Sn. Beyond the specific measurements of $B(E2, 0^+ \rightarrow 2^+)$ values, knowledge of the structure of the Sn isotopes is particularly important to test the neutron-neutron part of shell-model interactions as proton-proton and proton-neutron terms do not contribute at low energies and, therefore, low-lying states have a pure neutron character. The results of the two parts of experiment IS702 will aid the understanding of the evolution of neutron-neutron two-body matrix elements in nuclei with large neutron excess.

2 Status of IS702 and previous experiments

The first part of IS702, the Coulomb excitation of ^{130}Sn, has been performed in November 2022 as first experiment with the upgraded MINIBALL array after LS2. The set-up was identical to the one which is proposed in this addendum (see Section 3). A very preliminary Doppler-corrected spectrum is shown in Fig. 2
The obtained beam intensity from HIE-ISOLDE was about $5 \cdot 10^5$ pps at an energy of 4.4 MeV/u. ^{130}Sn was extracted from the production target as ^{130}Sn^{34}S^{+1} molecular ion which was cracked in the EBIS.

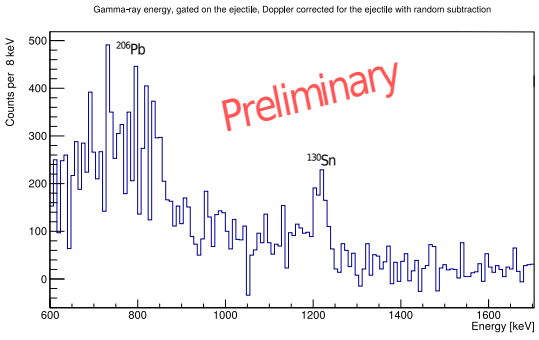

Figure 2: Preliminary γ-ray spectrum of ^{130}Sn after Doppler correction (courtesy of M. Droste).

The beam was impinging on a 2 mg/cm^2 thick ^{206}Pb target. The beam purity was $> 85\%$ with ^{130}Sb as dominant isobaric purity (a small contamination of ^{130}Te cannot be excluded at the current status of the analysis) and an isomeric ratio - g.s. compared to the 7^- isomer ($T_{1/2} = 1.7$ min) - of about 10%. The long-living daughter of the beam, ^{130}Sb ($T_{1/2} = 39.5$ min), caused background due to activation of the collimator upstream of the scattering chamber and the, by error in the beginning, not retracted Faraday cup downstream of the chamber. However, particle-γ coincidences cleaned the spectrum.

These data superseded in quality the data obtained in Coulomb excitation at the Holifield Radioactive Ion Beam Facility at ORNL where $B(E2, 0^+_{\text{g.s.}} \rightarrow 2^+_1)$ values for ^{128,130,132,134}Sn were determined and preliminary results reported [8, 9, 10].

The isotope ^{134}Sn was only measured with a BaF_2 array, efficient to cope with the low beam intensity, but only with moderate energy resolution. The authors pointed out that: 'This preliminary analysis does not yet include a complete experimental calibration of the photon detector efficiency.' [10]. The $B(E2, 0^+_{\text{g.s.}} \rightarrow 2^+_1)$ value reported for ^{134}Sn is 0.029(5) e^2b^2. The beam purity of ^{134}Sn amounted to 25% with a contamination of around 62% of ^{134}Te, 12% ^{134}Sb and 0.5% ^{134}Ba which complicated the analysis (see Fig. 3).

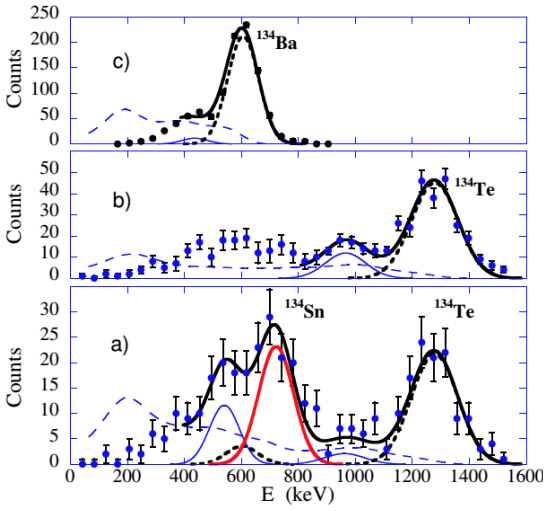

Figure 3: γ-ray spectrum recorded with the BaF_2 array TAMU after Coulomb excitation of ^{134}Sn (panel (a)). Contaminations stemming from ^{134}Ba and ^{134}Te (as demonstrated in panels (b) and (c), respectively) as well as two unidentified contributions (solid blue curve) are clearly visible. Figure from Ref. [8].

Recently, lifetimes of the 2^+_1, 4^+_1 and 6^+_1 states in ^{134}Sn have been measured at IDS applying the fast-timing method [3]. The extracted $B(E2, 0^+_{\text{g.s.}} \rightarrow 2^+_1)$ value of $0.0265^{+0.035}_{-0.0095}$ e^2b^2 is in agreement with the previous value, but the error is very large and does not allow for further evaluation in comparison with theory (see Fig. 1, right panel). On the other hand, the $B(E2, 4^+_1 \rightarrow 2^+_1)$ value, which is difficult for us (see Table 1), has been determined with high precision from the lifetime. Conclusively, the two experimental approaches are fully complementary.

3 Proposed experiment: 'safe' Coulomb excitation of ^{134}Sn

Coulomb excitation of the first excited 2^+ and 4^+ state in ^{134}Sn is proposed. The identical set-up, experimental method and analysis procedure was used by us for ^{130,132}Sn.

High beam intensities and purities for radioactive tin ions are based on molecular SnS beams. A post-accelerated beam at an energy of 4.4 MeV/u will be provided by HIE-ISOLDE allowing for the us of a high-Z target, i.e. ^{206}Pb, target for Coulomb excitation.

Large cross sections can be exploited for pure electromagnetic excitation at a distance of closest approach well above the criterion for 'safe' Coulex. The "safe" beam energy for ^{134}Sn on lead is about 4.4 MeV/u ($\vartheta_{\rm CM} = 180°$), calculated following Ref. [17].
The γ-rays from ^{134}Sn will be recorded with MINIBALL [18] and coincident scattered particles will be detected by a position sensitive double sided silicon detector (CD) in forward direction or, optionally, C-REX a version of T-REX [19] with a large angular coverage. The scattered ^{134}Sn ions are kinematically separated from the recoiling target nuclei at $\vartheta_{\rm Lab} < 70°$ even for target thicknesses of several mg/cm^2. This was calculated taking into account both the energy loss in the target from SRIM2008 [20] and the pulse height deficit [21]. This result was confirmed in our experiments, e.g. [7, 22].
The excitation cross section for Coulomb excitation depends not only on the transitional but also on the diagonal matrix elements, an effect known as reorientation. As the single- and multi-step processes and the reorientation effect depend on the scattering angle, a large coverage of scattering angles in the CM system is favourable. In the analysis, the data set is split in different angular bins. The matrix elements are then determined by a maximum likelihood fit.
The analysis of the excitation cross section will be performed relative to the excitation of the target. The cross section is maximised by using a high-Z ^{206}Pb target. The only state which will be excited ($E(2^+) = 803$ keV) is well separated from the expected γ-rays of ^{134}Sn (taking into account the effects caused by Doppler correction), which has the $2^+ \rightarrow 0^+$ transition at 725.6 keV and the $4^+ \rightarrow 2^+$ transition at 347.8 keV. The 3^- state in ^{206}Pb is above 2.6 MeV and decays by high-energy γ rays which do not overlap with the transitions of our interest.

	$15° < \vartheta_{\rm Lab,3} < 50°$ ($25° < \vartheta_{\rm CM} < 79°$)	$15° < \vartheta_{\rm Lab,4} < 50°$ ($80° < \vartheta_{\rm CM} < 149°$)
Ruth	42	3
2^+	0.42(4)	0.33(9)
4^+	0.0030(2)	0.011(3)
6^+	$6.5(5) \cdot 10^{-6}$	$1.0(1) \cdot 10^{-4}$

Table 1: *Calculated cross sections, in [b], for a ^{134}Sn beam at 588 MeV on a lead target. The impact by the reorientation effect is given in parentheses (see text).*

Table 1 summarises the calculated cross sections for elastic scattering and the excitation of the first three states in ^{134}Sn. The matrix elements are taken from theory, i.e. Ref. [13]. The $B(E2, 0^+_{\rm g.s.} \rightarrow 2^+_1)$ value lies well below the recent shell model prediction [2], but agrees with the existing experimental values. However, Ref. [13] (and all other calculations shown in Fig. 1, right panel, too) underpredicts the $B(E2, 2^+_1 \rightarrow 4^+_1)$ value (see fig. 1, right panel). Therefore, the cross sections given in Table 1 are to our best knowledge rather conservative values.
Different angular regions in the CM system are covered depending if the scattered projectile ($\vartheta_{\rm Lab,3}$) or the recoiling target ($\vartheta_{\rm Lab,4}$) is detected. The different sensitivities on single- or multi-step excitation at different CM scattering angle regions, e.g. the ratio $\sigma(4^+)/\sigma(2^+)$, are obvious. The impact of the reorientation effect is estimated assuming diagonal matrix elements of 0 eb and ± 0.5 eb for all states which results in cross section changes by up to 20%, in particular at backward CM angles. The diagonal matrix elements may be expected to be small, e.g. in ^{124,126,128}Sn values compatible with zero have been found [23]. However, for ^{134}Sn a quite large $Q_2(2^+_1) = 1.6$ eb is predicted [14].

The cross section for the ^{206}Pb target excitation is in the order of 0.5 b. For backward angles in the laboratory system which would be covered by C-REX too, much smaller cross sections are expected, compared to the forward region in the order of 10% and 25% for the 2_1^+ and 4_1^+ states, respectively. Hence, for this experiment the gain of using C-REX is quite small and does not justify the extra effort for setting it up. The main goal of this experiment, the determination of the $B(E2, 0^+_{\text{g.s.}} \rightarrow 2^+_1)$ value, can be achieved clearly with the forward CD alone. If a C-REX campaign would be performed, we would use it. As shown in Table 1, we expect that the 2_1^+ and, with very small cross section, the 4_1^+ state will be excited. Hence, the analysis described above has to consider only two transitional and two diagonal matrix elements. The isomeric 6^+ state has no impact. In addition, the $B(E2, 2_1^+ \rightarrow 4_1^+)$ value is now well-determined [3], hence its (small) impact due to interference terms in the excitation process is well under control. This allows to focus on our main target: **the determination of the $\mathbf{B(E2, 0^+_{g.s.} \rightarrow 2^+_1})$ value in ^{134}Sn**.
The beam composition will be determined from the characteristic γ-rays from the decay of the Sn, Sb, Te and Xe isotopes. For this purpose several techniques were established in previous MINIBALL experiments [7, 26, 27]. In 2022, additionally a HPGe detector was mounted next to the beamline after the HRS which measures the decay of the implanted beam halo [28]. From our experience with ^{A}Sn^{34}S^{+1} molecular beams, we expect as contaminants the respective A-isobars, mainly ^{A}Sb, and isotopes with A+34, in particular $^{A+34}$Yb [7, 27]. This isotope has been identified in the beam by the Coulomb excitation of its well-deformed ground state band. The isomeric 6^+ state in ^{134}Sn ($T_{1/2} = 81.7(12)$ ns [3]), if populated in the primary target, will decay completely before it could arrive at MINIBALL. However, the ground state of ^{134}Sn ($T_{1/2} = 1.05$ s [29]) (and its daughter ^{134}Sb) will decay to a small amount, about 10%, similar to ^{142}Xe ($T_{1/2} = 1.23$ s) measured 2016 [22, 26], inside the EBIS adding to the contamination.
The half-lives within the decay chain of ^{134}Sn (taken from [29]) are ^{134}Sb ($T_{1/2} = 0.78$ s), ^{134}Te ($T_{1/2} = 41.8$ min), ^{134}I ($T_{1/2} = 52.5$ min) and ^{134}Xe ($T_{1/2} > 5.8 \cdot 10^{22}$ y). As in the ^{130}Sn run, the long half-lives of the grand-daughter and beyond require similar care not to deposit activity around MINIBALL. However, activation by the long-lived decay products will decay within hours and is no issue for radiation protection.

4 Rate estimate and beam time request

The Sn isotopes of interest are produced using a standard UC$_x$/graphite target. Low-energy beams of neutron-rich Sn isotopes are available with highest intensity exclusively at HIE-ISOLDE. The strong Cs contamination is eliminated extracting SnS$^+$ molecules which are cracked afterwards in the EBIS. We will use isotopically enriched ^{34}S and produce a very clean $A = 168$ beam [30].
Latest ISOLDE yield measurements for Sn isotopes obtained reduced ion beam intensities compared to past experiments (see e.g. [31, 32]). A measured beam current of $3 \cdot 10^5$ ions/s was measured in 2016 for ^{132}Sn at the MINIBALL target [7]. This current value was a factor of 2-3 below the value extracted from the ISOLDE yield tables. In 2022, we obtained for ^{130}Sn an intensity of $\approx 5 \cdot 10^5$ pps which is roughly in agreement with the 10^6 pps estimated with this reduction factor and requested in the proposal [33]. Variations in

this order are not unexpected taking into consideration the different properties of the ISOLDE primary targets and the different HIE-ISOLDE settings. Therefore, we keep our request as in the proposal [33]. Assuming a proton current of 2 μA and, conservatively, an efficiency of HIE-ISOLDE of 5% the following **beam current is expected at the MINIBALL spectrometer: 10^4 ions/s for ^{134}Sn** (as requested for IS654 [27] too).
Slow extraction from the EBIS with pulse lengths of at least 1 ms is still desirable for this experiment to reduce the instantaneous particle rate.
Taking into account the integrated cross sections from Table 1, the count rate of the particle detector will be 5 counts/s corresponding which, of course, can be processed by the individual DSSSDs. The CD detector is divided in 2.5° bins (annular strips). Hence, the obtained statistics should allow to split the data set in angular bins adapted to scattered projectiles and recoiling target nuclei.
With the expected beam current and the integrated cross sections from Table 1 the γ-particle coincidence rates and the expected statistics are given in Table 2. A ^{206}Pb target of 4 mg/cm^2 thickness (e.g. the same target as for IS548 [26, 22]) was assumed. Energy dependent MINIBALL detection efficiencies are taken from [18].

transition	counts/hour	counts/run
$2_1^+ \rightarrow 0^+_{\text{g.s.}}$	15	1800
$4_1^+ \rightarrow 2_1^+$	0.3	34

Table 2: *Calculated particle-γ-ray yields following Coulomb excitation of ^{134}Sn. Right column assumes 15 shifts of beam time.*

The **requested 18 shifts** will be divided into **15 shifts for beam on target** (rightmost column in Table 2) and **3 shifts for a careful diagnosis of the beam composition**. The requested shifts will allow to determine the $\mathbf{B(E2; 0^+_{gs} \rightarrow 2^+_1)}$ and $B(E2; 2_1^+ \rightarrow 4_1^+)$ values with statistical errors ≈2% and ≈17%, respectively. The total error of the $B(E2; 0^+_{\text{gs}} \rightarrow 2^+)$ value of the previous experiment was 17% [10]. **We aim to improve the total error to below 5%**. The impact of the diagonal matrix elements (not discussed in [10]) will be included in our analysis. This would increase the tension between experiment and the recent shell model calculations [2] and would allow to evaluate other theory predictions which differ by about 30% (Fig. 1, right panel).
In this way, the electric quadrupole moment Q_2 of the 2_1^+ state can be extracted too, although we expect a large experimental uncertainty. However, for short-lived states this quantity is only accessible by safe Coulomb excitation via reorientation and cannot be obtained directly by any other method, e.g. fast-timing experiments. The $B(E2; 2^+ \rightarrow 4^+)$ value will have a larger error compared to the value from a fast-timing measurement [3] because of the expected low statistics. Here, only the consistency can be checked and the large difference between calculations and experimental value seen in Fig. 1 can be supported or questioned. Potentially, a candidate for the first 3^- octupole state could be observed adding to a comprehensive understanding of this neutron-rich region. However, from our results for the 3^- state in ^{142}Xe [22] we do not expect an octupole collectivity large enough allowing for an observation with the available beam intensities.
The measurement of the $B(E2, 0^+_{gs} \rightarrow 2^+)$ values in both neighbours of the doubly-magic ^{132}Sn will be crucial for understanding the nuclear structure of Sn isotopes around the $N = 82$ shell closure and an experimental benchmark for theory.

In total we ask 18 (15+3) shifts for ^{134}Sn.

References

[1] I. Arcavi *et al.*, Nature 551, 64 (2017); M. R. Drout *et al.*, Science 10.1126/science.aaq0049 (2017); many more.

[2] T. Togashi *et al.*, Phys. Rev. Lett. 121, 062501 (2018).

[3] M. Piersa-Siłkowska *et al.*, Phys. Rev. C 104, 044328 (2021).

[4] J. Cederkäll *et al.*, Phys. Rev. Lett. 98, 172501 (2007).

[5] A. Ekström *et al.*, Phys. Rev. Lett. 101, 012502 (2008).

[6] P. Doornenbal *et al.*, Phys. Rev. C 78, 031303(C) (2008).

[7] D. Rosiak *et al.*, Phys. Rev. Lett. 121, 252501 (2018).

[8] J. R. Beene *et al.*, Nucl. Phys. A 746, 471c (2004).

[9] D. C. Radford *et al.*, Nucl. Phys. A 752, 264c (2005).

[10] R. L. Varner *et al.*, Eur. Phys. J. A 25, s01, 391 (2005).

[11] J.Terasaki, J.Engel, W.Nazarewicz, M.Stoitsov, Phys. Rev. C 66 (2002) 054313.

[12] S. Sarkar and M. Saha Sarkar, Phys. Rev. C 78, 024308 (2008).

[13] M. P. Kartamyshev et al., Phys. Rev. C 76, 024313 (2007).

[14] A. Covello et al., J. Phys.: Conf. Ser. 267, 012019 (2011).

[15] J. D. Holt et al., J. Phys. G: Nucl. Part. Phys. 39, 085111 (2012).

[16] S. Sarkar and M. Saha Sarkar, J. Phys.: Conf. Ser. 267, 012040 (2011).

[17] H. J. Wollersheim, Habilitation Treatise (Universität Frankfurt/Main, 1993).

[18] N. Warr et al., Eur. Phys. J. A 49, 40 (2013).

[19] V. Bildstein et al., Eur. Phys. J. A 48, 85 (2012).

[20] J. F. Ziegler, `http://www.srim.org`

[21] G. Pasquali et al., Nucl. Instr. Meth. A 405, 39 (1998).

[22] C. Henrich, doctoral thesis (TU Darmstadt, 2021).

[23] J. M. Allmond et al., Phys. Rev. C 84, 061303(R) (2011).

[24] U. C. Bergmann et al., Nucl. Instr. Meth. B 204, 220 (2003).

[25] J. Terasaki Phy. Rev. C 66, 054313 (2002).

[26] Th. Kröll et al., CERN-INTC-2019-011 / INTC-SR-070.

[27] Th. Kröll et al., CERN-INTC-2019-006 / INTC-SR-065.

[28] U. Koester, private communication.

[29] `http://www.nndc.bnl.gov`.

[30] U. Koester et al., Nucl. Instr, Meth. B 266, 4229 (2008).

[31] Th. Kröll et al., CERN-INTC-2012-042 / INTC-P-343.

[32] T. Stora, private communication.

[33] P. Reiter, Th. Kröll et al., CERN-INTC-2021-039 / INTC-P-608.

Appendix

DESCRIPTION OF THE PROPOSED EXPERIMENT

The experimental setup comprises:

Part of the	Availability	Design and manufacturing
(fixed ISOLDE installation: MINIBALL + only CD, or MINIBALL + C-REX)	☒ Existing	☒ To be used without any modification
[^{134}Sn experiment/ equipment]	☒ Existing	☒ To be used without any modification ☐ To be modified
	☐ New	☐ Standard equipment supplied by a manufacturer ☐ CERN/collaboration responsible for the design and/or manufacturing

HAZARDS GENERATED BY THE EXPERIMENT (if using fixed installation:) Hazards named in the document relevant for the fixed [MINIBALL + only CD, MINIBALL + T-REX] installation.

Additional hazards:

Hazards	[Part 1 of experiment/ equipment]	[Part 2 of experiment/ equipment]	[Part 3 of experiment/ equipment]
Thermodynamic and fluidic			
Pressure	[pressure][Bar], [volume][l]		
Vacuum			
Temperature	[temperature] [K]		
Heat transfer			
Thermal properties of materials			
Cryogenic fluid	[fluid], [pressure][Bar], [volume][l]		
Electrical and electromagnetic			
Electricity	[voltage] [V], [current][A]		
Static electricity			
Magnetic field	[magnetic field] [T]		
Batteries	☐		
Capacitors	☐		
Ionizing radiation			
Target material [material]			

Beam particle type (e, p, ions, etc)	^{134}Sn		
Beam intensity at MINIBALL	10^4 ions/s		
Beam energy	4.4 MeV/u		
Cooling liquids	[liquid]		
Gases	[gas]		
Calibration sources:	☐		
• Open source	☐		
• Sealed source	☒ [ISO standard]		
• Isotope standard sources	^{60}Co, ^{152}Eu		
• Activity (sources are available)			
Use of activated material:			
• Description	☐		
• Dose rate on contact and in 10 cm distance	[dose][mSV]		
• Isotope			
• Activity			
Non-ionizing radiation			
Laser			
UV light			
Microwaves (300MHz-30 GHz)			
Radiofrequency (1-300 MHz)			
Chemical			
Toxic	[chemical agent], [quantity]		
Harmful	[chem. agent], [quant.]		
CMR (carcinogens, mutagens and substances toxic to reproduction)	[chem. agent], [quant.]		
Corrosive	[chem. agent], [quant.]		
Irritant	[chem. agent], [quant.]		
Flammable	[chem. agent], [quant.]		
Oxidizing	[chem. agent], [quant.]		
Explosiveness	[chem. agent], [quant.]		
Asphyxiant	[chem. agent], [quant.]		
Dangerous for the environment	[chem. agent], [quant.]		
Mechanical			

Physical impact or mechanical energy (moving parts)	[location]		
Mechanical properties (Sharp, rough, slippery)	[location]		
Vibration	[location]		
Vehicles and Means of Transport	[location]		
Noise			
Frequency	[frequency],[Hz]		
Intensity			
Physical			
Confined spaces	[location]		
High workplaces	[location]		
Access to high workplaces	[location]		
Obstructions in passageways	[location]		
Manual handling	[location]		
Poor ergonomics	[location]		

Hazard identification:

none